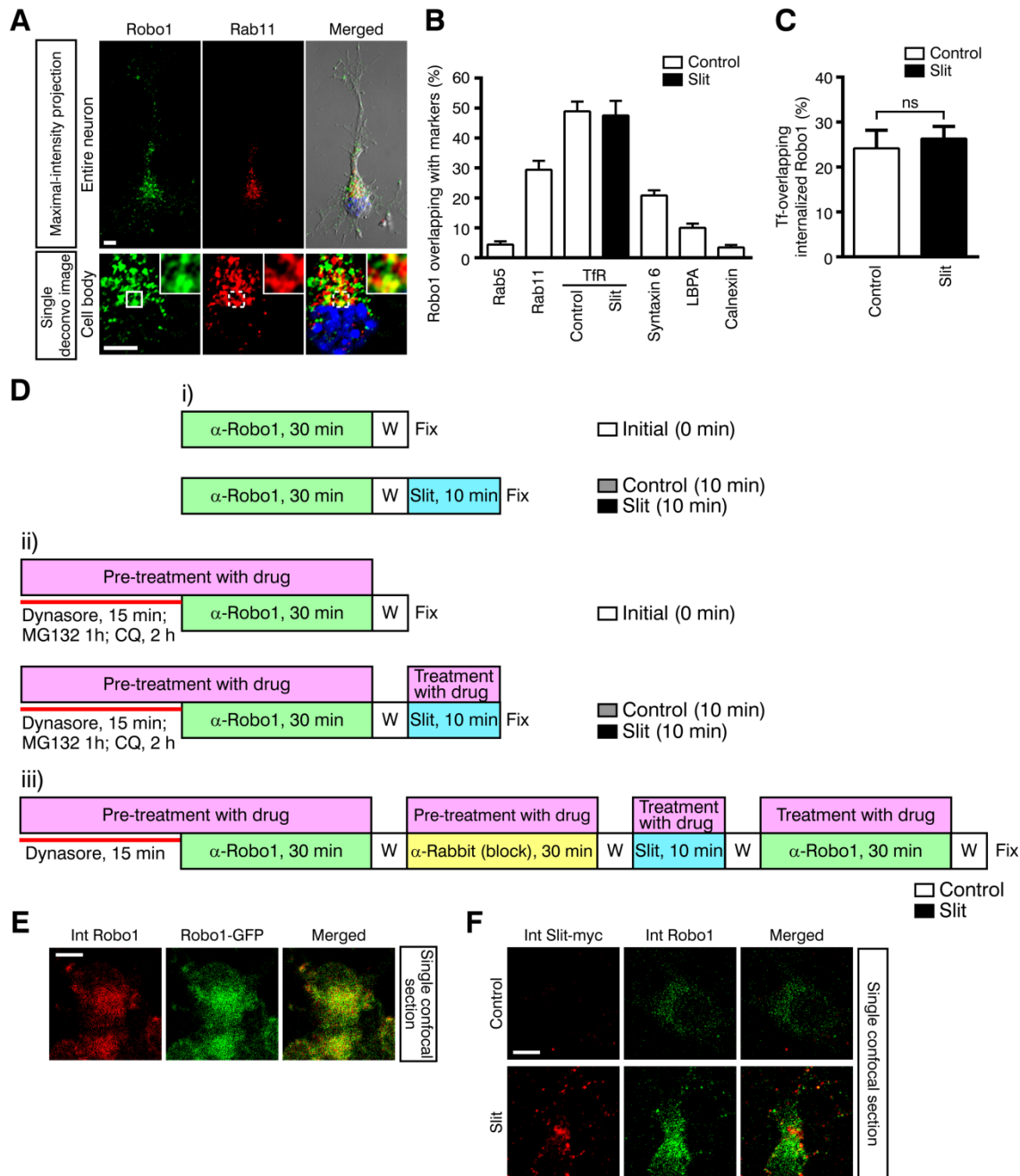
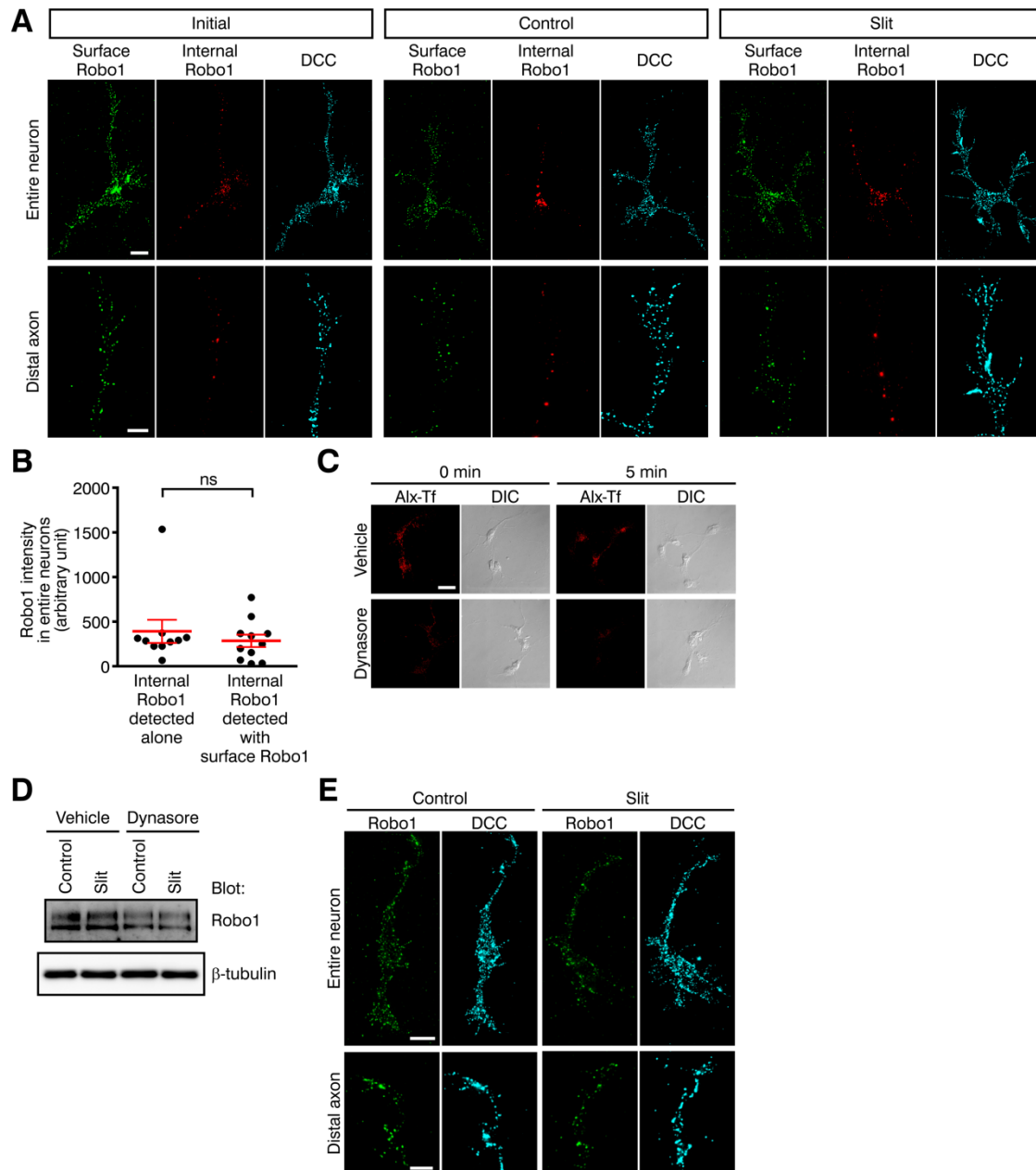


**Figure S1. Robo1 expression and dynamics in commissural neurons.** (A) Co-immunostaining of Robo3 (green) and DCC (red) (left) or Robo1 (green) and TAG-1 (red) (right) in E11.5 dorsal spinal cord neurons. Differential interference contrast (DIC) images are also shown. (B) Co-immunostaining of Robo1-HA [C-terminally hemagglutinin (HA)-tagged]–expressing HEK293 cells with anti-Robo1 (green) and anti-HA (red) antibodies (left panel). Right panel: spatial pixel intensity correlations between anti-Robo1 and anti-HA signals. Pearson's correlation coefficient ( $r$ ) is shown. (C) Subcellular distribution of Robo1 (green) in E9.5 DCC<sup>+</sup> (red) commissural neurons stimulated with 25 pM Slit for 10 min. The images were taken under the same conditions as in Fig. 1A. (D) The merged images of E11.5 triple-labelled [Robo1 (green)/DCC (red)/Hoechst33342 (blue)] commissural neurons shown in Fig. 1A. A small fraction of Robo1 exhibited an overlap with DCC. (E) Comparison of Robo1 immunosignal intensity per area of the entire neuron between E9.5 and 11.5 DCC<sup>+</sup> commissural neurons stimulated with the control. Here and in subsequent figures, mean  $\pm$  SEM is presented.  $n = 30$  (neurons) (10 neurons/experiment, 3 independent experiments). \*\*\* $P < 0.001$ ; two-tailed Mann-Whitney test. (F) DCC levels in the distal axon of commissural neurons stained as in Fig. 1A.  $n = 30$  (neurons) (10 neurons/experiment, 3 experiments).  $P = 0.2011$ ; Mann-Whitney test. ns: not significant. (G) Western blot analysis showing Robo1 protein expression in E11.5 dorsal spinal cord neurons stimulated with 25 pM Slit or control for 10 min. The overall levels of Robo1 were not affected by Slit during the time frame of our observation. (H) Cell-surface biotinylation of Robo1 in primary dorsal spinal cord neurons prepared from E12.5 mouse embryos. Neurons were stimulated with 25 pM Slit for 10 min. Extracellular domains were biotinylated for 30 min on ice, and the biotinylated proteins were recovered by pulldown using avidin-agarose and subjected to Western blot analysis. (I) Live-cell imaging of the axon of a Robo1-GFP-expressing dorsal spinal cord neuron cultured from E11.5 embryos. The neuron was imaged before and after Slit stimulation (25 pM). The growth cone is marked with red arrows. Scale bars, 10  $\mu$ m (A–D,I). All immunofluorescence images were acquired using an Olympus BX61I epifluorescence microscope and deconvoluted. Robo1 and TAG-1 immunostaining images in (A) were denoised using Sefir software before deconvolution.



**Figure S2. Robo1 localization in the endocytic recycling compartment and schemes of live-cell antibody-feeding assays.** (A) Endogenous Robo1 exhibits a partial overlap with Rab11 in E11.5 dorsal spinal cord neurons. Images composed of green (Robo1), red (Rab11), blue (Hoechst 33342) and DIC channels and magnified views are shown. (B) Percentages of Robo1-positive pixels overlapping with organelle markers in the cell body were quantified. Lysobisphosphatidic acid (LBPA) and calnexin were used as markers for late endosomes and the endoplasmic reticulum, respectively.  $n = 10, 10, 11, 11, 11, 10$  and  $10$  (neurons) from left to right. (C) Quantification of percentages of Alexa555-Tf-overlapping, internalized Robo1 in neurons immunostained as in Fig. 2D.  $n = 10$

(neurons).  $P = 0.4727$ ; Mann-Whitney test. ns: not significant. (D) Time course of drug treatment and antibody-labelling in antibody-feeding assays shown in Fig. 2E. (E) The distribution of anti-Robo1 antibody (red) internalized after surface-labelling in E12.5 primary dorsal spinal cord neurons expressing Robo1-GFP (green). (F) Slit-binding assay in E12.5 primary dorsal spinal cord neurons. Partially overlapping distribution of internalized Slit2-myc (red, detected with anti-myc) and internalized Robo1 (green). Scale bars, 5  $\mu\text{m}$  (A,E,F). Images in (A) were acquired using an Olympus BX61I epifluorescence microscope and deconvoluted. Images in (E,F) were obtained with a Zeiss LSM710 confocal microscope.



**Figure S3. Differential detection of surface, internal and freshly surface-inserted Robo1 in antibody-feeding assays.** (A) Robo1 immunostaining in vehicle-treated neurons stained as in Fig. 2E-ii). Maximal-intensity projections of deconvoluted Z-stacks are shown. Neurons were incubated with anti-Robo1 and stimulated with 25 pM Slit or control for 10 min before fixation and differential detection of surface (green) and internal (red) Robo1. DCC expression is shown in cyan. (B) Comparison of signal intensity per area between internal Robo1 levels detected alone and those detected simultaneously with surface Robo1. Both of the internal Robo1 levels were measured in entire neurons that were stimulated with control for 10 min after labelling with anti-Robo1. ‘Internal Robo1 levels detected alone’ were quantified in the neurons in which surface Robo1 was blocked with unconjugated anti-rabbit secondary antibody. ‘Internal

Robo1 levels detected simultaneously with surface Robo1 levels' were quantified in the neurons stained as in Fig. 2E-ii).  $n = 11$  (neurons).  $P = 0.6433$ . ns: not significant. (C) Suppression of Tf uptake in commissural neurons by treatment with dynasore. Maximal-intensity projections of deconvoluted Z-stacks together with DIC images are shown. Neurons were treated with 40  $\mu\text{M}$  dynasore (the same concentration as used in Fig. 2G) or vehicle for 30 min, incubated with Alexa555-conjugated Tf (red) for 10 min at 16°C, transferred back to 37°C and kept for the indicated times. The neurons were acid-washed before fixation to remove surface-bound Tf. (D) Western blot analysis showing Robo1 protein expression in E11.5 dorsal spinal cord neurons treated with vehicle or dynasore, stimulated with 25 pM Slit or control for 10 min. (E) Freshly surface-inserted Robo1 (green) in  $\text{DCC}^+$  (cyan) commissural neurons stained as in Fig. 2E-iii). Maximal-intensity projections of deconvoluted Z-stacks are shown. Surface Robo1 was blocked with anti-Robo1 and unconjugated secondary antibodies, stimulated with Slit or control for 10 min and re-incubated with anti-Robo1 to detect freshly surface-inserted Robo1. Scale bars, 10  $\mu\text{m}$  (top panels) and 5  $\mu\text{m}$  (bottom panels) (A); 20  $\mu\text{m}$  (C); 10  $\mu\text{m}$  (top panels) and 5  $\mu\text{m}$  (bottom panels) (E). All immunofluorescence images were acquired using an Olympus BX61I epifluorescence microscope and deconvoluted.

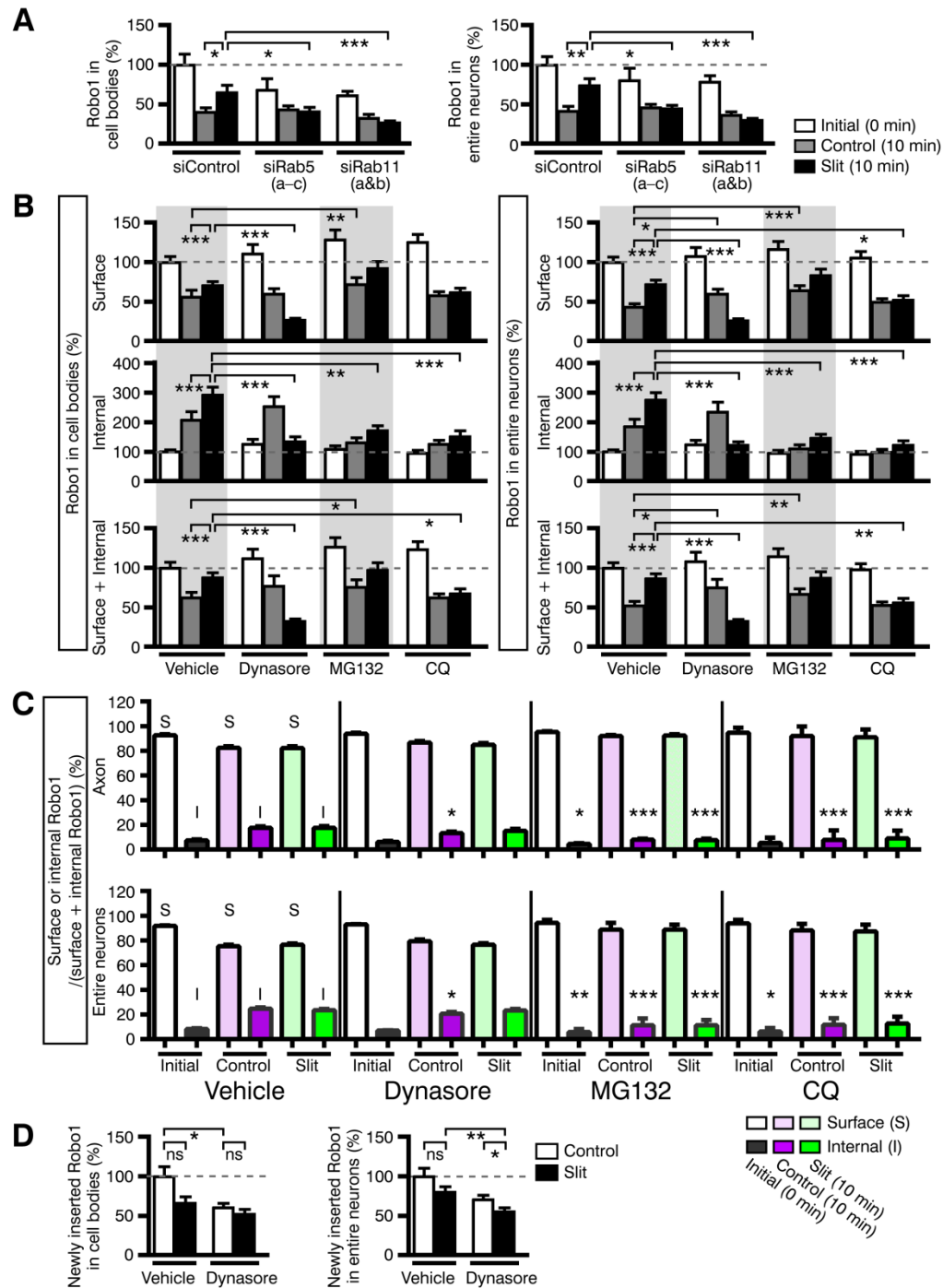


**Figure S4. Slit-induced Robo1 endocytic recycling in commissural neurons.** (A) Effects of RNAi of Rab5 or Rab11 on Robo1 levels in the cell body and entire neuron [stained as in Fig. 2E-i]. *n*-values are given in the legend of Fig. 2F. \**P* < 0.05; \*\**P* < 0.01; \*\*\**P* < 0.001; Mann-Whitney test. (B) Quantification of surface, internal and surface + internal levels of antibody-labelled Robo1 in the cell body and entire neuron [stained as in Fig. 2E-ii) and Fig. S3A]. Robo1 levels in drug-treated neurons were compared to those of vehicle-treated neurons before stimulation (initial). See also Fig. 2G.

(C) Quantification of the two ratios, surface Robo1/(surface + internal Robo1) and internal Robo1/(surface + internal) Robo1, in the distal axon and entire neuron. Endocytosis of antibody-labelled Robo1 that have occurred immediately after the antibody-labelling step (0 min) or 10 min after stimulation were quantified. The initial ratios of internal Robo1/(surface + internal) Robo1 were designated as background levels of internalized Robo1 (see black bars).  $*P < 0.05$ ;  $**P < 0.01$ ;  $***P < 0.001$  (vs. corresponding vehicle-control); Mann-Whitney test. (D) Quantification of Robo1 insertion from the cytoplasm to the surface of the cell body and entire neuron [stained as in Fig. 2E-iii) and Fig. S3E]. Robo1 levels were compared to that of vehicle-treated, control-stimulated neurons. See also Fig. 2H. ns: not significant.

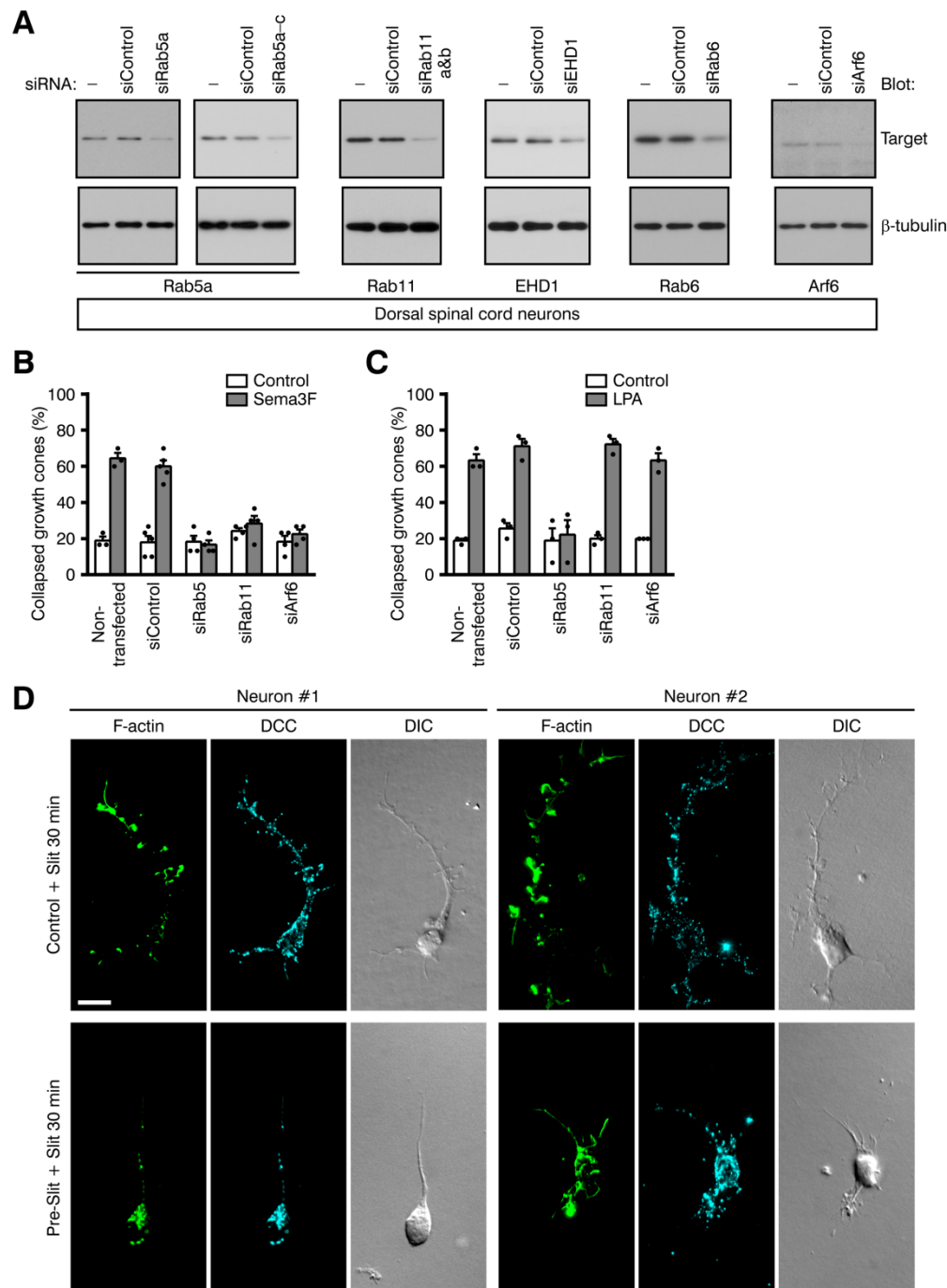


**Figure S5. Growth cone collapse responses of commissural neurons to repellents.**

(A) siRNA-mediated knockdown of endocytic recycling regulators used in this study. Western blot analysis showing that siRNAs targeting Rab5, Rab11, EHD1, Rab6 or Arf6 suppressed expression of the corresponding endogenous protein in primary dorsal spinal cord neurons from E11.5–12.5 embryos following transfection.  $\beta$ -tubulin was used as a loading control. Note that Western blot analyses were performed by using the entire population of cultured neurons including non-transfected neurons and siRNA-transfected ones, whereas the growth cone collapse phenotypes were scored by analysing DCC-

positive neurons successfully transfected with siRNA (shown by red fluorescence of Alexa555-conjugated RNA oligo). (B,C) Growth cone collapse of siRNA-transfected E11.5–12.5 commissural neurons in response to Sema3F (B) or LPA (C) were examined as in Fig. 3A–C (stimulation with 100  $\mu$ g/ml Sema3F or 1  $\mu$ M LPA for 30 min). In (B),  $n = 3, 5, 4, 4$  and  $4$  (experiments) from left to right (30 neurons/experiment). In (C),  $n = 3$  (experiments). (D) Slit-sensitized commissural neurons. Neurons were pre-stimulated with 5 pM Slit or control for 30 min, and further stimulated with 25 pM Slit for 30 min, as in Fig. 3D. Neurons were visualized by staining with Alexa488-conjugated phalloidin (green) and anti-DCC (cyan). Two neurons per group are shown. Slit sensitization drastically affected the morphology of the growth cone, axon and cell body. In Slit-sensitized neurons (bottom panels), growth cone structures were completely lost, and the number of lateral extensions and the axon length were reduced, as compared with unsensitized neurons (top panels). Scale bar, 10  $\mu$ m. Images in (D) were acquired using an Olympus BX61I epifluorescence microscope and deconvoluted.

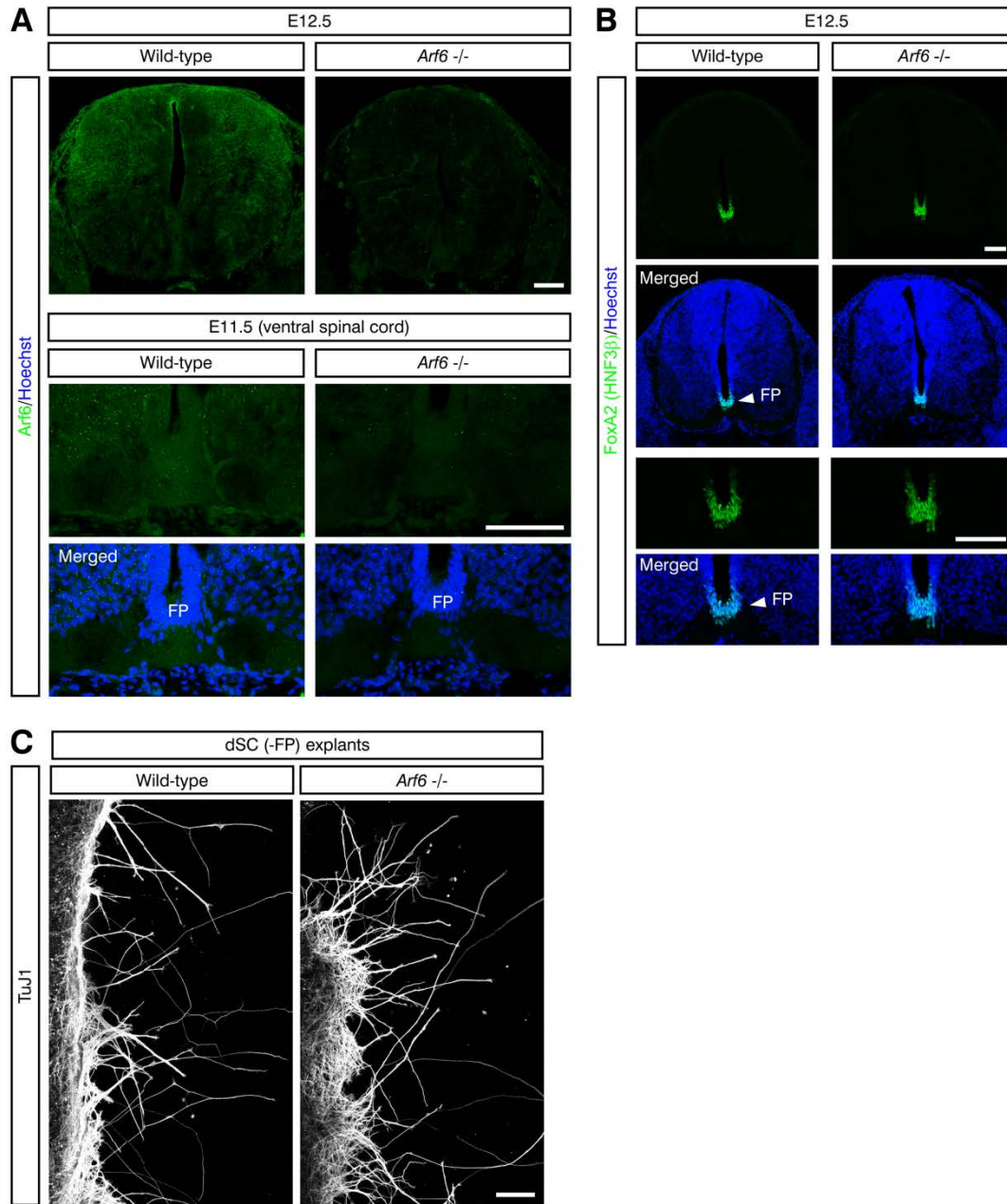


**Figure S6. Immunohistochemistry for *Arf6* and *FoxA2*, and spinal cord explants in *Arf6*<sup>-/-</sup> mutants.** (A) Immunohistochemistry for *Arf6* of spinal cord sections of E12.5 wild-type and *Arf6*<sup>-/-</sup> littermates (top panels). *Arf6* distribution was detected in the midline-crossing commissural axon region in E11.5 ventral spinal cords (bottom panels). (B) Immunohistochemistry for *FoxA2*/HNF3β in E12.5 spinal cords. The expression patterns appeared indistinguishable between wild-type and *Arf6*<sup>-/-</sup> spinal cords. (C) TuJ1 immunostaining of explant cultures of E11.5 dorsal spinal cords. Scale bars, 100 μm (A–C). All images were acquired using a Zeiss LSM780 confocal microscope.

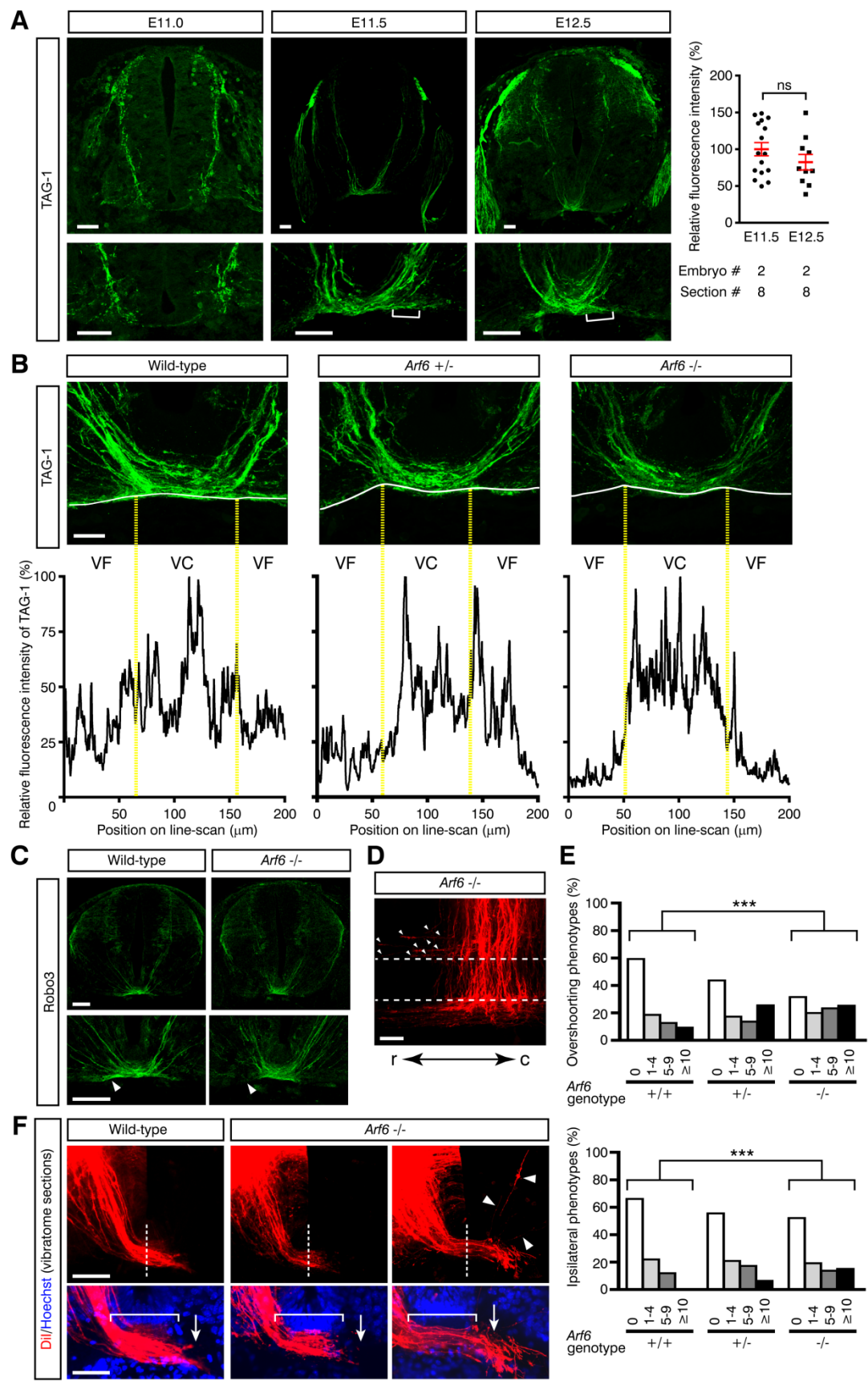


**Figure S7. Immunohistochemistry for TAG-1 and Robo3, and DiI labelling in *Arf6*<sup>-/-</sup> mutants.** (A) TAG-1 immunohistochemistry in brachial-level spinal cords at E11.0, E11.5 and E12.5 (left panel). Right panel: quantification of TAG-1 immunofluorescence in the mVF (white brackets in left panels).  $P = 0.2249$ ; Mann-Whitney test. ns: not significant. (B) Relative fluorescence intensity profiles of TAG-1 immunostaining in the spinal cords shown in Fig. 5A. Bottom graphs are line-scans, revealing relative fluorescence intensity of TAG-1 immunosignals through the VF and VC, along the white lines shown in the top panels. (C) Robo3 distribution in E12.5 wild-type and *Arf6*<sup>-/-</sup> spinal cords at the brachial level. Arrowheads show the mVF region. In wild-type embryos, Robo3 was highly expressed in the pre- and midline-crossing axon segments, but downregulated after midline crossing. In *Arf6*<sup>-/-</sup> mutants, Robo3 expression in the mVF was lower than that in wild-type embryos. (D) An additional example of anterograde DiI labelling of dorsal commissural axons in E12.5 *Arf6*<sup>-/-</sup> spinal cords. Axon stalling at the midline and ipsilateral turning were observed (some ipsilateral axons were marked with arrowheads). r: rostral; c: caudal. (E) Quantification of overshooting (top) and ipsilateral (bottom) phenotypes in commissural axons in E12.5 *Arf6*<sup>-/-</sup> mutants examined by anterograde DiI labelling. Percentages of phenotypes showing indicated numbers of overshooting or ipsilateral axons per DiI injection site are presented as open, shaded and solid black bars.  $n$ -values are given in the legend of Fig. 5E. \*\*\* $P < 0.0001$ ;  $\chi^2$  test. (F) DiI labelling of commissural axons in transverse vibratome sections of E12.5 spinal cords. In the top panels, the midline is shown by dashed lines, and in the bottom panels, the FP is marked with brackets. In wild-type embryos, commissural axons crossed the FP, turning longitudinally on the contralateral side (marked with an arrow; most growth cones disappeared from the image planes after FP crossing). In *Arf6*<sup>-/-</sup> mutants, many axons were stalled within the FP or at the contralateral FP edge, and the stalled growth cones were visible in these regions on the equivalent image planes; some axons aberrantly entered the contralateral grey matter after FP crossing (arrowheads). Scale bars, 50  $\mu\text{m}$  (A); 25  $\mu\text{m}$  (B); 100  $\mu\text{m}$  (C); 50  $\mu\text{m}$  (D); 100  $\mu\text{m}$  (top panels) and 50  $\mu\text{m}$  (bottom panels) (F). All immunofluorescence images were acquired using a Zeiss LSM780 confocal microscope.

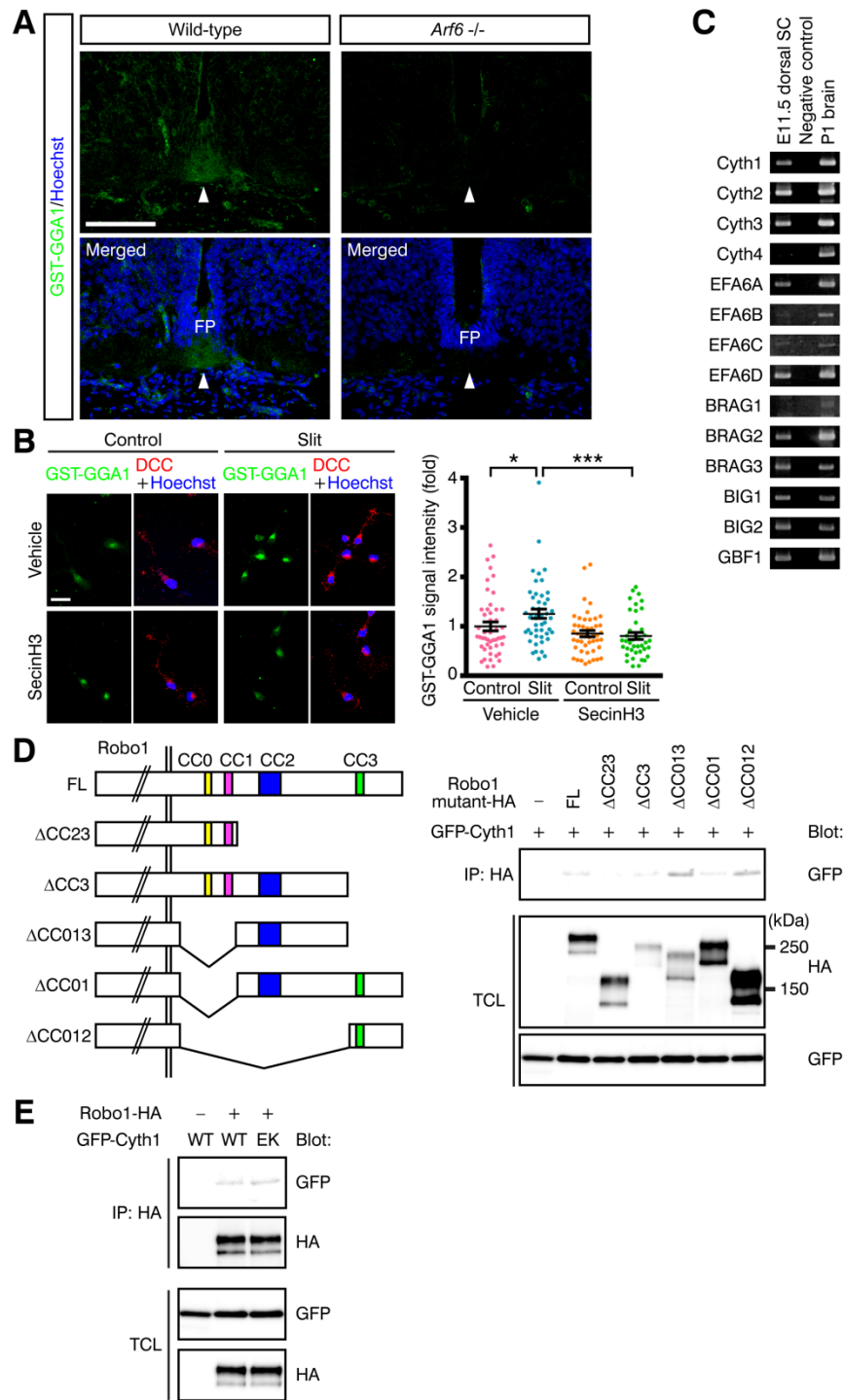


**Figure S8. Slit activation of Arf6 in commissural neurons, expression of Arf-GEFs and Robo1-cytohesin interactions.** (A) GST-GGA1 immunolabeling of spinal cord sections of E12.5 wild-type and *Arf6*<sup>-/-</sup> littermates. Active Arf GTPases were detected by GST-GGA1. The midline is marked with arrowheads. (B) GST-GGA1 immunolabeling (green) in E12.5 commissural neurons (DCC<sup>+</sup>; red) stimulated with 25 pM Slit or control for 20 min in the presence or absence of SecinH3. The right graph shows quantification

of GST-GGA1 signal intensity (4 experiments; 10 or more neurons/experiment).  $n = 48$ , 48, 47 and 40 (neurons) from left to right.  $*P = 0.0156$ ;  $***P = 0.0001$ ; Mann-Whitney test. (C) RT-PCR analysis of mRNA expression of Arf-GEFs in E11.5 dorsal spinal cord (SC) neurons. cDNA prepared from postnatal day 1 (P1) whole-brain was used as a positive control. Negative control: PCR without template cDNAs. (D,E) Co-immunoprecipitation was carried out using lysates of HEK 293 cells co-transfected with HA-tagged Robo1 and GFP-tagged Cyth1. Lysates of the transfected cells were immunoprecipitated with anti-HA. The immunoprecipitates and total cell lysates (TCL) were probed with antibodies as indicated by Western blotting. IP: immunoprecipitation. (D) Co-immunoprecipitation of HA-tagged Robo1 deletion mutants with GFP-Cyth1 in HEK293 cells. The left panel shows a schematic illustration of full-length (FL) and deletion mutants of rat Robo1. Residues 1099 to 1657 were deleted in  $\Delta$ CC23; residues 1455–1657 were deleted in  $\Delta$ CC3; residues 930–1098 and 1455–1657 were deleted in  $\Delta$ CC013; residues 930–1098 were deleted in  $\Delta$ CC01; residues 930–1454 were deleted in  $\Delta$ CC012. The right panel shows that the CC2 and CC3 motifs of Robo1 mainly contribute to the Robo1-Cyth1 interaction. (E) Co-immunoprecipitation of Robo1-HA with wild-type or catalytically inactive forms of GFP-Cyth1. Scale bars, 100  $\mu$ m (A); 20  $\mu$ m (B). All immunofluorescence images were acquired using a Zeiss LSM780 confocal microscope.

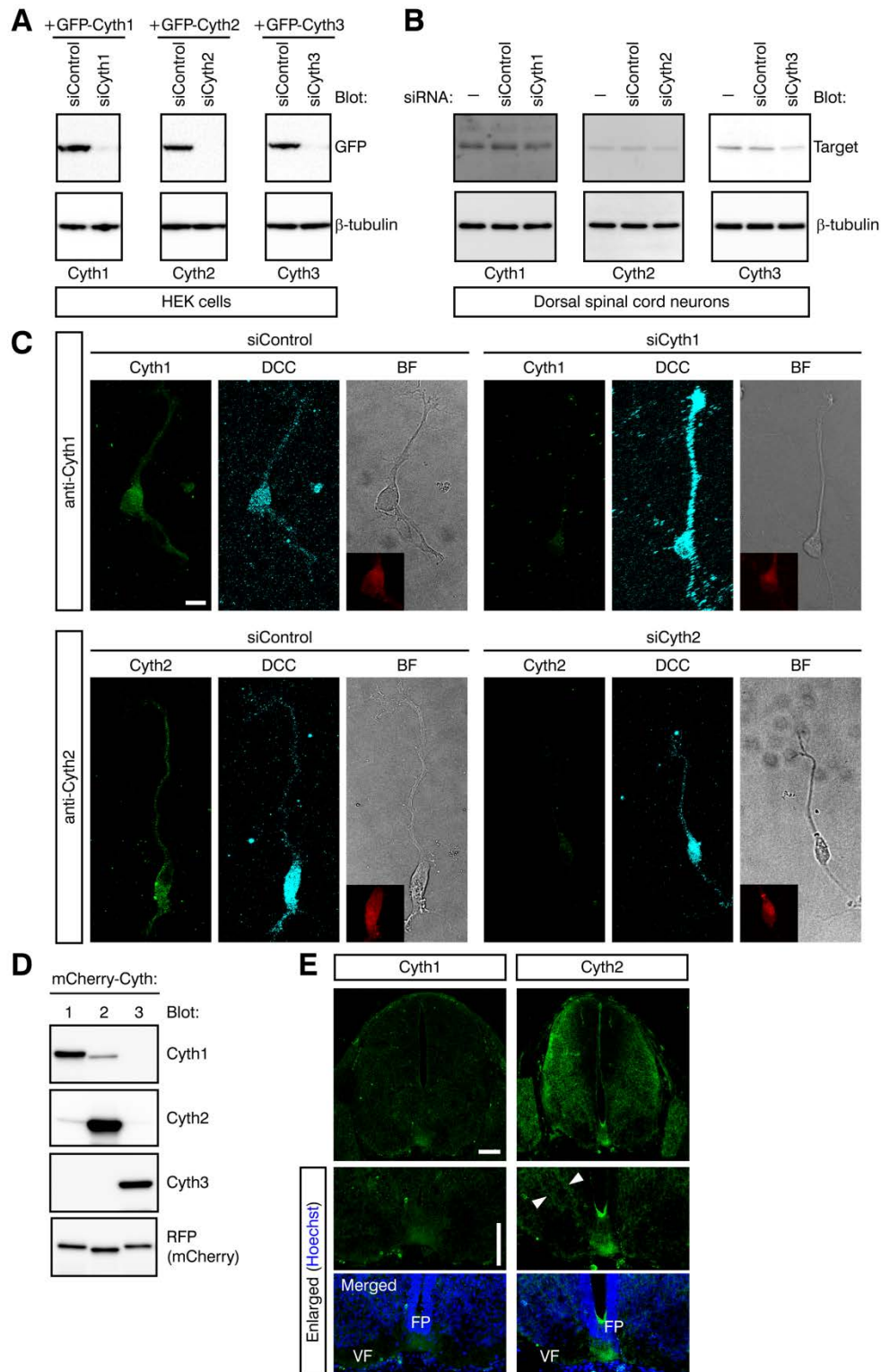


**Figure S9. RNAi of cytohesins and immunostaining.** (A,B) Western blot analysis showing that siRNA-mediated knockdown of Cyth1–3 suppressed expression of GFP-tagged mouse Cyth1–3 in HEK293 cells (A) and endogenous Cyth1–3 in primary dorsal

spinal cord neurons from E11.5–12.5 embryos (B). (C) Immunocytochemistry with anti-cytohesin antibodies showing that expression of Cyth1 and Cyth2 proteins (green) in E12.5 DCC<sup>+</sup> (cyan) commissural neurons was suppressed by siRNA transfection. Maximal-intensity projections of confocal Z-stacks together with bright field (BF) images are shown. The efficient introduction of siRNAs into commissural neurons was visualized by fluorescence of Alexa555-conjugated RNA oligo in the soma (red signals in the insets). (D) The specificity of anti-cytohesin antibodies. HEK 293 cells were transfected with plasmids expressing mCherry-tagged cytohesins, and the cell lysates were immunoblotted with the antibodies indicated. (E) Confocal microscopy of expression patterns of Cyth1 and Cyth2 in E12.5 spinal cords. Scale bars, 10  $\mu$ m (C); 100  $\mu$ m (E). Images in (C) and (E) were acquired using Leica TCS SP8 and Zeiss LSM780 confocal microscopes, respectively.

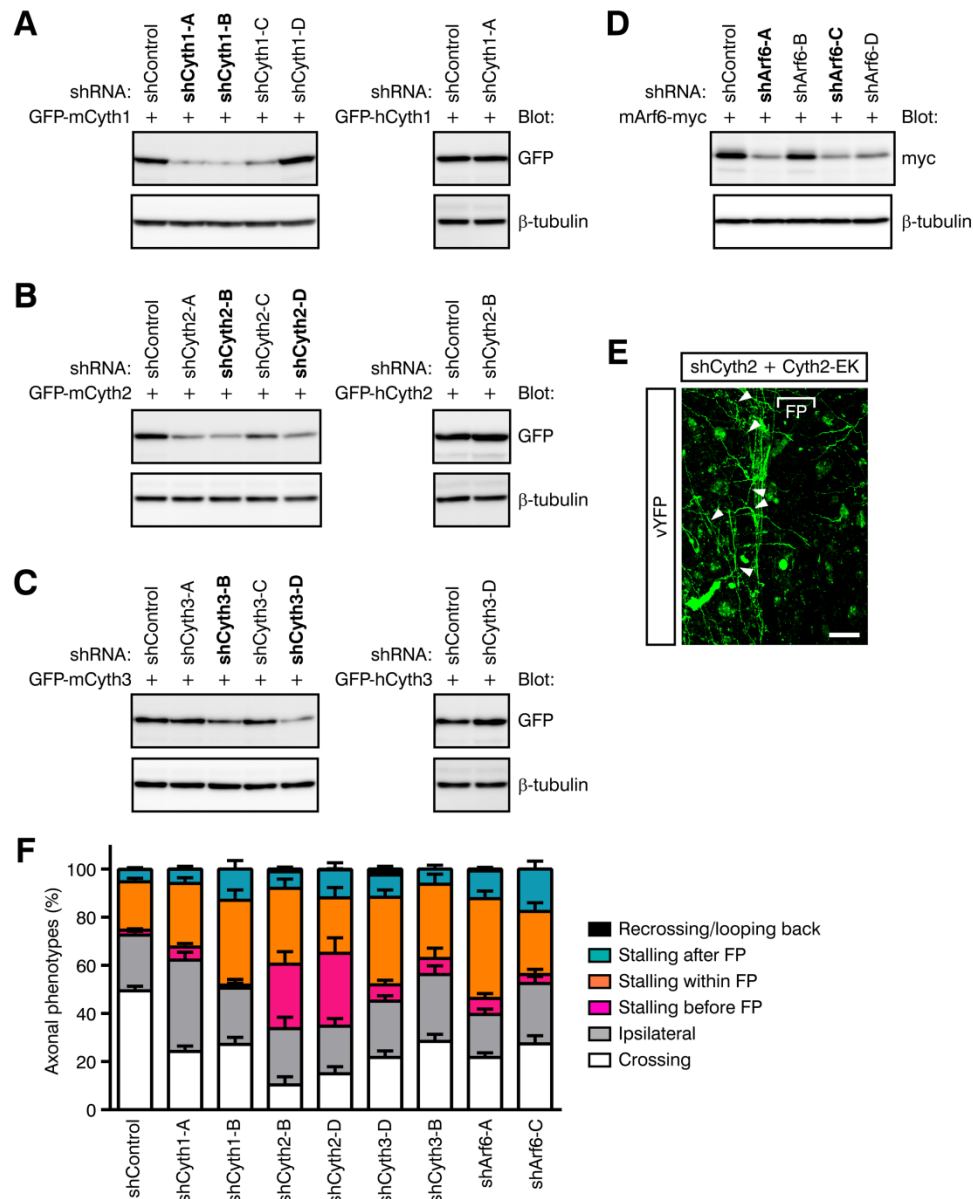


**Figure S10. Roles of cytohesin-Arf6 pathways in midline axon pathfinding.** (A–D) Western blot analysis showing that shRNAs to Cyth1 (A), Cyth2 (B), Cyth3 (C) or Arf6 (D) suppressed the expression of GFP-tagged mouse cytohesin or myc-tagged Arf6 in HEK293 cells. The shRNAs shown in bold were used in *ex vivo* electroporation. (E) Midline axon trajectories of neurons co-electroporated with shCyt2, vYFP and Cyt2-E156K plasmids in the spinal cord. Arrowheads show ipsilaterally turning axons. (F) Quantification of effects of two independent sequences of shRNAs against *cytohesins* or *Arf6* on midline axon pathfinding in spinal cord explants. Combined results for the two sequences of shRNAs against each cytohesin or Arf6 are shown in Fig 7C. shCyt1-A, shCyt2-B and shCyt3-D were used for rescue experiments by co-introducing shRNA-resistant human cytohesin expression plasmids.  $n = 91, 30, 14, 23, 23, 21, 12, 33$  and  $12$  (imaging fields) from left to right. Scale bar, 50  $\mu$ m (E). The image in (E) was acquired using a Zeiss LSM780 confocal microscope.

**Table S1**

<b>List of PCR primers for detecting expression of mouse Arf-GEFs</b>
<p><b>Cyth1</b>                      (Forward) TTGCTAATGAAATTGAAAGCCTGGGAT                      (Reverse) TTCATGGCGATGAATCTCTCCACCGTA</p>
<p><b>Cyth2</b>                      (Forward) AAGTGAAGCTATGAGCGAGGT                      (Reverse) TTCATGGCCACAAAGCGCTCCAGG</p>
<p><b>Cyth3</b>                      (Forward) ATTGACAACCTGACTTCAGTG                      (Reverse) ATGGTGATGAAGCGCTCAGCGGTG</p>
<p><b>Cyth4</b>                      (Forward) TGTTTGCCCAAATCGACTGCT                      (Reverse) TCCTCTACCTTCTGCACGGAG</p>
<p><b>EFA6A</b>                      (Forward) CTGTGGGGACTTCATCGGAAA                      (Reverse) TGATCCAGGACTGCATTGCT</p>
<p><b>EFA6B</b>                      (Forward) CATCAGAGCCCTCAAACCTCTGGAC                      (Reverse) GAAGCCAAGTGAACATGGTGCTGG</p>
<p><b>EFA6C</b>                      (Forward) ACATGGATGAAGAGAAGCTCCCATGTG                      (Reverse) CAGGCCATCCTTAAGGCTGGTGTCAC</p>
<p><b>EFA6D</b>                      (Forward) ATGAGAAGAAGCCGAACGTGT                      (Reverse) GCCGCGGATGGATTCTAAGTA</p>
<p><b>BRAG1</b>                      (Forward) ATCTATCGGGATAAGGAGCGA                      (Reverse) CGAAGTATGCAGGGTTCTGTG</p>
<p><b>BRAG2</b>                      (Forward) GCTTTCAGCAACGATGTCATC                      (Reverse) CACGTGGTCCTCGTTGGTCTT</p>
<p><b>BRAG3</b>                      (Forward) ACGCTCTCCACAGACACCCTG</p>

(Reverse) ACAGCACCGTCTTCATGCCCA

GBF1

(Forward) AGAAGGCACAGCTTTGGTTCC

(Reverse) GCCAGGTCTGGCTGTCTCTTT

BIG1

(Forward) GATGTCTGGCACTGATAATCC

(Reverse) TTATACAGAAGTCGTCTTTGC

BIG2

(Forward) TTCAGGATGACCCAGAGCAGT

(Reverse) ACATTGTACAGCAGCCGCCTC

---

**Table S1.** PCR primers used in RT-PCR analysis of Arf-GEFs expression in dorsal spinal cord neurons

## Supplemental Materials and Methods

### Animals

For timed-pregnancy mating, the day of vaginal plug observation was dated as E0.5, and embryos were staged as described (Yuasa-Kawada et al. 2009a). CD1 (ICR) mice (Charles River and Kyudo) and *Arf6* knockout mice (Suzuki et al. 2006) maintained on the C57BL/6J background were used.

### Antibodies, DNA constructs and reagents

Antibodies against Robo1 (rabbit polyclonal, a gift from Drs A. Tamada and F. Murakami), Cyth1 (rabbit polyclonal, a gift from Dr J. Ikenouchi), Cyth2 (rabbit polyclonal, a gift from Dr S. Bourgoin), EHD1 (rabbit polyclonal, a gift from Dr S. Caplan), *Arf6* (mouse monoclonal, 3A-1, a gift from Dr S. Bourgoin, and rabbit polyclonal) and lysobisphosphatidic acid (LBPA) (mouse monoclonal, 6C4, a gift from Dr J. Gruenberg) were used for immunostaining and Western blotting. Commercially available mouse monoclonal antibodies used in this study were: anti-DCC (AF5; Calbiochem/Merck Millipore), anti-L1 (2C2; Abcam; ab24345), Alexa647-conjugated anti- $\beta$ 3-tubulin (TuJ1; BD), anti-transferrin receptor (TfR) (H68.4; Thermo Fisher Scientific), anti-HA.11 (Covance), anti- $\beta$ -tubulin (TUB2.1; Sigma-Aldrich), anti-Rab5 (15/Rab5; BD), anti-Rab11 (47/rab11; BD), anti-syntaxin 6 (30/Syntaxin 6; BD), TAG-1 (4D7; Developmental Studies Hybridoma Bank) and Alexa488-conjugated anti-GST (#617234; Merck Millipore). The rat monoclonal antibodies anti-L1 (324; Merck Millipore) and anti-HA (3F10; Roche), the rabbit polyclonal antibodies anti-Robo1 (RP2791; ECM Biosciences and 20219-1-AP; Proteintech), anti-Rab5 (isoform-specific; 11947-1-AP, 27403-1-AP; Proteintech), anti-Rab6 (10187-2-AP; Proteintech) and HRP-conjugated anti-RFP (PM005-7; MBL) and the rabbit monoclonal antibodies anti-FoxA2/HNF3 $\beta$  (D56D6; Cell Signaling Technology) and anti-Cyth3 (EP394Y; Gene Tex) were also used. Alexa-conjugated secondary antibodies and Alexa-conjugated phalloidin and transferrin (Tf) were purchased from Thermo Fisher Scientific. Sema3F protein was purchased from R&D Systems. LPA, dynasore, MDC, MG132 and chloroquine were from Sigma-Aldrich/Merck. SecinH3 was obtained from Merck Millipore.

Green fluorescent protein (GFP)-tagged rat Robo1 was subcloned into pCS2<sup>+</sup> vector. Wild-type and constitutively inactive, GFP-tagged human Rab5a and Rab11a constructs were gifts from Drs M. Zerial and M. Ehlers. HA-tagged human *Arf6*, GST-GGA1 and mCherry-tagged human Cyth1–3 plasmids were gifts from Dr K. Nakayama. myc-tagged mouse *Arf6* construct was also used to test efficiencies of sh*Arf6*. cDNAs encoding mouse Cyth1–3 were obtained from MGC (Mammalian Gene Collection) clones BC057974, BC004662 and BC035296 (transOMIC technologies). GFP-tagged mouse and human wild-type Cyth1–3 were constructed by using PCR with these plasmids as templates. Catalytically inactive, GFP-tagged human Cyth1-E157K, Cyth2-E156K and Cyth3-E161K mutants were generated by site-directed mutagenesis (QuikChange Lightning kit; Agilent Technologies). For rescue experiments in Fig 6C, siCyth2-resistant, GFP-tagged wild-type and mutant Cyth2 constructs were generated by introducing silent mismatches through site-directed mutagenesis. Robo1 deletion mutants

have been previously described (Yuasa-Kawada et al. 2009a; Wong et al., 2001). *Venus-YFP* (vYFP) cDNA was subcloned into pCAG vector to generate pCAG-vYFP.

### Cell culture and Slit stimulation

Primary neuronal cultures were prepared from E9.5 or E11.5–12.5 dorsal spinal cords, as previously described (Yuasa-Kawada et al., 2009a). Briefly, neurons were plated on coverslips pre-coated with poly-D-lysine (50 µg/ml, Sigma) and laminin (5 µg/ml, Roche) in Dulbecco's modified Eagle medium (DMEM) supplemented with 10% fetal bovine serum. When purified recombinant Slit2 was used for stimulation of neurons, culture media were replaced with Neurobasal supplemented with B-27 (Thermo Fisher Scientific) on the next day after plating. Neurons were cultured for 2 days in vitro (DIV2; a total of 48 h) before Slit stimulation.

HEK293 cells stably expressing human Slit2-myc or rat Robo1-HA have been described previously (Li et al., 1999). The cell lines have been routinely tested and found negative for mycoplasma contamination. Stimulation of neurons with Slit was as described previously (Yuasa-Kawada et al., 2009a). Slit2 proteins were purified by ion-exchange chromatography using SP-sepharose FF (GE Healthcare) (Guan et al., 2007). Control conditioned media or purified preparations, which were made from parental HEK cells by employing the same procedure as for Slit, were used for the assays in parallel. For Fig. 1A–D and 3, and Fig. S1B–F and S5D, Slit-conditioned media were used; for Fig. 1F,G, 2 and 6, and Fig. S1G,H, S2, S3, S4 and S8B, purified Slit protein was used. In all experiments, Slit was added to the medium to give a final working concentration of 25 pM, except for sensitization assays (Fig. 3E–G and Fig. S5D).

### Explant culture

Dorsal parts of spinal cords or intact floor plate (FP)-including half parts (from the cervical to lumbar levels) were dissected out from E11.5 embryos and the pial membrane was removed in  $\text{Ca}^{2+}$ – $\text{Mg}^{2+}$ -free Hanks' solution (HCMF) (see Fig. 1E). With modifications from protocols for retinal explants (Halfter et al. 1983), spinal cords were spread onto black nitrocellulose filters (Sartorius) precoated with 125 µg/ml concanavalin A (Sigma), with the pial side downward and with an extra care taken not to include any FP tissues into the explant (for dorsal spinal cord explants). The filters mounted with spinal cord explants were then reversed, held onto Matrigel (BD; diluted in HCMF to 10% (v/v))-coated coverslips with two metal weights, without embedding in collagen. The explants were cultured with the ventricular side in contact with the surface of the coverslip in a 1:1 mixture of Neurobasal + B-27 and DMEM (Thermo Fisher Scientific) + FBS media for 48 h. Factors to enhance axon growth from spinal cord explants, such as netrins, were not included in our cultures. The cultures were treated with Slit for 10 min and fixed for immunostaining.

### siRNAs and shRNAs

Duplex siRNAs to mouse-specific sequences were obtained from Dharmacon, they were as follows: siControl (ON-TARGETplus siCONTROL Non-targeting siRNA #1: D-001810-01), siRobo1#1 (ON-TARGETplus J-046944-10) (Yuasa-Kawada et al., 2009a), pools containing four different sequences of siRNAs against *Rab5* (5a: ON-TARGETplus SMARTpool L-040855-00, 5b: L-040856-01, 5c: L-040857-01, Dharmacon), *Rab6* (ON-

TARGETplus SMARTpool L-040858-01), *Rab11* (11a: ON-TARGETplus SMARTpool L-040863-01, 11b: L-040864-01), *EHD1* (ON-TARGETplus SMARTpool L-040747-01), *Arf6* (ON-TARGETplus SMARTpool L-043217-01), *Cytl1* (ON-TARGETplus SMARTpool L-058480-01) and *Cyth3* (ON-TARGETplus SMARTpool L-062720-01). siCyth2 (Silencer Select, Ambion/Thermo Fisher Scientific) was as previously described (Li et al., 2012). For *ex vivo* electroporation into spinal cords, shRNAs against mouse *Cytl1*, *Cyth2*, *Cyth3* and *Arf6* (in pRS shRNA vector; Origene) were used. Control shRNA (shControl) was also obtained from Origene.

To perform RNAi in dissociated, dorsal spinal cord neurons, a total of 90 pmol of non-labelled siRNAs were mixed with 40 pmol of Block-iT Alexa Fluor Red Fluorescent Control (Thermo Fisher Scientific) and transfected into the neurons ( $1.0 \times 10^6$  cells) resuspended in Opti-MEM (Thermo Fisher Scientific) using 2  $\mu$ l of Lipofectamine RNAiMAX (Thermo Fisher Scientific) at 37°C for 75 min. Subsequently, the neurons were washed twice before plating, and cultured for 48 h before Slit stimulation. For rescue experiments, siRNA-introduced neurons were re-transfected with plasmids encoding siRNA-resistant, GFP-tagged wild-type or mutant human Rab5a, Rab11a or cytohesins by using Lipofectamine LTX (Thermo Fisher Scientific) on the next day after plating, according to the manufacturer's protocol, and subjected to assays one day later. In the rescue experiments to verify the specificity of siRNA- or shRNA-mediated knockdown of cytohesins, we used constructs encoding the most abundant isoform of cytohesin in the fetal brain: Cytl1 and Cyth2 with GGG motif, and Cyth3 with GG motif (Ogasawara et al. 2000).

### Live-cell antibody-feeding assays

Different types of live-cell antibody-feeding assays were performed by using our previously published protocol with minor modifications (Yuasa-Kawada et al., 2009a). For live-cell immunocytochemistry (Fig. 1B, 6D), neurons were stimulated with Slit or control for 10 min, washed once with fresh Neurobasal media supplemented with 20 mM HEPES (Thermo Fisher Scientific), incubated with a rabbit anti-Robo1 antibody (2  $\mu$ g/ml) (Long et al., 2004; Tamada et al., 2008; Yuasa-Kawada et al., 2009a) for 30 min at room temperature, washed and fixed. Samples were permeabilized and stained with anti-DCC and Alexa-conjugated secondary antibodies.

For Fig. 2D, cultured neurons were incubated with rabbit anti-Robo1 and Alexa555-conjugated Tf (50  $\mu$ g/ml) for 30 min at room temperature, in order to label Robo1 and the ERC, respectively. After washing, neurons were stimulated with Slit or control for 10 min at 37°C and fixed. The surface Robo1 was blocked with unconjugated anti-rabbit secondary antibody (10  $\mu$ g/ml; Thermo Fisher Scientific). After permeabilization, internalized Robo1 was detected with Alexa488-conjugated anti-rabbit secondary antibodies. Neurons were also labelled with mouse anti-DCC and Alexa647-conjugated anti-mouse secondary antibodies.

For the live-cell antibody-feeding assay shown in Figs. 2E-i) and 2F, neurons were stained using the same protocol as described previously (Yuasa-Kawada et al., 2009a). Briefly, surface Robo1 was labelled with rabbit anti-Robo1-extracellular domain (2  $\mu$ g/ml) in fresh culture media supplemented with 20 mM HEPES for 30 min at room temperature. After extensive washing with fresh media, the neurons were immediately fixed (to monitor the initial levels of Robo1 before stimulation), or stimulated with Slit or

control for 10 min and fixed. After permeabilization with 0.2% Triton X-100 in PBS for 2 min, the fixed neurons were immunostained with anti-DCC and Alexa-conjugated secondary antibodies.

For the antibody-feeding assay shown in Fig. 2E-ii) and 2G, neurons were pretreated with dynasore (Macia et al., 2006) (40  $\mu$ M; 15 min), MG132 (20  $\mu$ M, 1 h), chloroquine (100  $\mu$ M; 2 h) or vehicle control, and further treated during the subsequent steps, including antibody-feeding and Slit stimulation, until fixation (see Fig. S2D). Surface Robo1 was labeled with rabbit anti-Robo1 for 30 min at 16°C (to reduce endocytosis). After extensive washing, the neurons were immediately fixed, or stimulated with Slit or control for 10 min at 37°C and fixed. To discriminate between surface Robo1 and internalized Robo1, surface Robo1 (green) was first reacted by incubation of the fixed neurons with Alexa488-conjugated anti-rabbit secondary antibodies without permeabilization for 3 h at room temperature. After three washes with PBS and permeabilization with 0.2% Triton X-100 in PBS for 2 min, the neurons were immunolabeled with mouse anti-DCC for 2 h at room temperature and then with Alexa647-conjugated anti-mouse secondary antibodies and Alexa555-conjugated anti-rabbit secondary antibodies for 2 h at room temperature to visualize DCC (cyan) and internalized Robo1 (red). To calculate surface + internal Robo1 levels, multiple sets of the same types of samples (non-treated neurons before stimulation) were processed in parallel and immunostained for surface Robo1 (green) and internal Robo1 (red) or vice versa. Levels of green and red immunosignals of internal Robo1 were then compared to obtain the ratio of green signals to red signals. Finally, the internal Robo1 levels were obtained on the base of green signals, and the surface + internal levels were calculated.

For the antibody-feeding assay shown in Fig. 2E-iii) and 2H, to visualize newly surface-inserted Robo1, neurons were incubated with rabbit anti-Robo1 (2  $\mu$ g/ml; it was confirmed that this concentration was saturating for Robo1 immunostaining) for 30 min at 16°C, washed, subjected to incubation with an excess amount of unconjugated anti-rabbit Fab fragment (described as "Blocking" in Fig. 2E; used at 10  $\mu$ g/ml; Jackson ImmunoResearch) for 30 min at 16°C to block surface-remaining Robo1 before Slit stimulation and then washed. The neurons were stimulated with Slit or control for 10 min at 37°C, washed and re-incubated with rabbit anti-Robo1 for 30 min at 16°C. After washing, the neurons were fixed, and freshly surface-inserted populations of Robo1 were labelled with Alexa488-conjugated anti-rabbit secondary antibodies. The neurons were permeabilized and incubated with mouse anti-DCC and then with Alexa647-conjugated anti-mouse secondary antibodies. In a negative control experiment, neurons that were live-labelled with rabbit anti-Robo1 and blocked with the unconjugated anti-rabbit Fab were fixed immediately at 0 min (namely without 10-min stimulation). To verify the efficiency to mask initially surface-resident Robo1, such neurons were incubated with Alexa488-conjugated secondary antibodies, without the permeabilization step, and no significant Robo1 signal was detected.

For Fig. S3C, Tf uptake assay was performed as described (Macia et al., 2006).

### **Growth cone collapse assays and GST-GGA1 immunolabeling**

Slit-, Sema3F- or LPA-stimulated growth cone collapse assays were performed as described previously (30 min stimulation except for Slit sensitization assays) (Yuasa-Kawada et al., 2009a). Sema3F protein or LPA was used at 100  $\mu$ g/ml or 1  $\mu$ M,

respectively. Growth cones were defined by the presence of lamellipodia and/or filopodia. Neurons were selected randomly based on fluorescence of anti-DCC and/or Block-iT Alexa Fluor Red Fluorescent Control. For drug-treatment experiments, neurons were pre-incubated with dynasore (40  $\mu$ M; 15-min pretreatment), MDC (10 nM; 30-min pretreatment), SecinH3 (10  $\mu$ M; 30-min pretreatment) or vehicle control (the maximal concentrations for each drug that did not affect growth cone morphology in commissural neurons in the absence of Slit were determined). Subsequent growth cone collapse assays were performed in the presence of the drug. In each experimental group, at least three independent experiments were performed (30 neurons per group were scored in each experiment).

For GST-GGA1 immunolabeling, neurons were stimulated as indicated, fixed, treated with 50 mM  $\text{NH}_4\text{Cl}$  and permeabilized with 0.2% Triton X-100 in PBS. Neurons were then immunolabeled as described with some modifications (Harrington et al., 2011). Briefly, neurons were incubated with 8  $\mu$ g/ml purified GST-GGA1 probe overnight at 4°C. The neurons were washed and incubated with anti-DCC for 2 h at room temperature, and with Alexa555-conjugated anti-mouse secondary antibodies for 2 h at room temperature, followed by incubation with Alexa488-conjugated anti-GST antibody for 2 h at room temperature. Z-stack images were taken with an LSM780 microscope, summed and quantified.

### Immunohistochemistry

Embryos were fixed overnight at 4°C in 4% PFA/PBS, washed with PBS, incubated in 5% and 30% sucrose/PBS overnight and embedded in a mixture of OCT and 30% sucrose/PBS (the volume ratio of 3:1). Spinal cord transverse cryosections at brachial to abdominal levels (20  $\mu$ m) were collected on Superfrost glass slides (Matsunami) and air-dried overnight. The slides were used directly for immunostaining or kept at -80°C until use. Slides were blocked in PHT (0.1% Triton X-100 in PBS containing 1% heat-inactivated goat serum) for 1 h at room temperature, incubated with the primary antibody in PHT overnight at 4°C, washed 3 times with PBS, incubated with the secondary antibody in PHT for 2 h at room temperature, washed 3 times with PBS and coverslip-mounted with Permafluor (Thermo Fisher Scientific). For immunostaining for Cyth1 and Cyth2, cryosections were unmasked by microwave irradiation in 10 mM citric acid (pH6.0). All controls were wild-type littermates of the mutant embryos.

Images were taken with an LSM780 microscope, and quantitative analyses were performed by an individual blind to the genotype, using MetaMorph software. For quantification of immunoreactivity of TAG-1 and Robo1 in the medial ventral funiculus (mVF), the signal intensity in a rectangular region (100 x 15  $\mu$ m) was measured on both sides of a brachial-level spinal cord section per embryo after background subtraction and threshold setting, and then normalized to the mean intensity obtained from each of the age-matched wild-type littermate embryos.

For GST-GGA1 immunolabeling, cryosections were blocked as described above, and incubated with 8  $\mu$ g/ml purified GST-GGA1 probe overnight at 4°C and with Alexa488-conjugated anti-GST antibody for 2 h at room temperature.

## DiI labelling

Spinal cords of E12.5–14.5 wild-type and *Arf6*<sup>-/-</sup> embryos were fixed in an open-book configuration with 4% PFA/PBS overnight. Alternatively, transverse vibratome sections (100 µm-thick) of E12.5 embryos were prepared (wild-type: *n* = 4; *Arf6*<sup>-/-</sup>: *n* = 3). For anterograde axon labelling, the dorsal spinal cords were injected with small crystals of DiI (Thermo Fisher Scientific) and the DiI was allowed to diffuse for two days to label commissural axons anterogradely along their entire length. For retrograde axon labelling, the VF regions of spinal cords were injected with DiI crystals and the DiI was allowed to diffuse for three days to label ipsilateral axons and contralateral commissural axons, as well as their cell bodies. Samples were observed with an LSM710 or LSM780 microscope.

## Cell-surface biotinylation, Arf6 pulldown assays, co-immunoprecipitation and Western blotting

Cell-surface biotinylation, Arf6 pulldown assays, co-immunoprecipitation and Western blotting were performed essentially as described in previous studies (Hanai et al., 2016; Santy and Casanova, 2001; Yuasa-Kawada et al., 2009a, 2009b).

Briefly, cell-surface biotinylation in primary dorsal spinal cord neurons from E12.5 embryos was performed by using the Cell Surface Protein Isolation kit (Pierce/ThermoFisher Scientific). After a brief wash with ice-cold PBS following stimulation, cells were incubated in 250 µg/ml EZ-Link-Sulfo-NHS-SS-Biotin for 30 min at 4°C. Addition of a quenching solution containing glycine terminated the biotinylation reaction. Cells were then washed with cold Tris-buffered saline and lysed in a buffer (50 mM Tris-HCl, pH7.4, 150 mM NaCl, 1% Triton X-100) containing a protease inhibitor cocktail (Roche). Lysates were then incubated with Neutravidin-agarose at 4°C overnight, and biotinylated proteins were subsequently eluted from the beads by heating at 95°C for 5 min in 2x Laemmli buffer with 50 mM DTT.

To monitor Arf6 activation in response to Slit in control or Robo1-HA-expressing HEK293 cells, human wild-type Arf6-HA-expressing plasmid was transfected. After serum starvation for 16 h, cells were stimulated with Slit for the indicated times and lysed. Active, GTP-bound Arf6 was captured with GST-GGA1 (Hanai et al., 2016; Santy and Casanova, 2001) and detected by immunoblotting with anti-Arf6. For Arf6 pulldown in primary cultures of mouse cortical neurons, the endogenous active Arf6 was detected with anti-Arf6. For co-immunoprecipitation between Robo1 and cytohesins in the cell extracts prepared from embryonic mouse whole-brain, including the hindbrain and rostral spinal cord (from the cervical to brachial levels), Robo1 protein was immunoprecipitated with a rabbit polyclonal antibody against the C-terminal domain of Robo1 (ECM Biosciences) in a buffer containing 1% NP-40 and 1% sodium deoxycholate and detected by immunoblotting with another anti-Robo1 rabbit polyclonal antibody (Proteintech). Pulldown samples, immunoprecipitates and cell lysates were resolved on an SDS-PAGE gel, immunoblotted and detected with ECL Plus, ECL Prime, ECL Select, ECL Advance kit (GE Healthcare) or Western Lightening ECL Pro (Perkin Elmer) using the X-ray films, LAS3000 or LAS4000mini (GE Healthcare). Can Get Signal kit (Toyobo) was used for detecting weak immunosignals.

## RT-PCR

Total RNA was extracted from cultured dorsal spinal cord neurons from E11.5 embryos by using Illustra RNAspin mini RNA isolation kit (GE Healthcare) and reverse-transcribed with Superscript reverse transcriptase II (Thermo Fisher Scientific) and random primer at 42°C for 60 min. cDNAs were subjected to 33 cycles of PCR, each cycle consisting of 95°C for 2 min, 95°C for 30 sec, 56°C (Cyth1, Cyth3, BRAG1–3, EFA6A and EFA6C) or 60°C (Cyth2, Cyth4, EFA6B, EFA6D, GBF1, BIG1 and BIG2) for 30 sec and 74°C for 60 sec, followed by 74°C for 10 min, using Ex Taq polymerase. The primers used are listed in Table S1.

## *Ex vivo* electroporation and spinal cord explant culture

Spinal cords of E11.5 embryos were injected with a solution containing shRNA constructs (2 µg/µl) and pCAG-vYFP (0.4 µg/µl). For rescue experiments, GFP-tagged, human wild-type or catalytically inactive mutant cytohesin expression plasmid (1 µg/µl) was co-introduced into the embryos. Immediately thereafter, embryos were electroporated with three 50-ms pulses of 20 V at 50-ms intervals using NEPA21 (NEPA GENE) and forceps-type electrodes (CUY665P9-6-2-5). The spinal cords were dissected out, and their ‘closed-book’ preparations were covered with collagen matrix (Koken) and cultured in media consisting of 45% Opti-MEM I, 50% F-12, 40 mM glucose and 5% horse serum (Sabatier et al., 2004) (see Fig. 7A). After culturing for 4 days (with media change daily) and dissecting out from the collagen gel, the spinal cords were fixed in an open-book configuration with 4% PFA/PBS. Confocal Z-stacks of green-channel images for visualizing vYFP signals and differential interference contrast (DIC) images were taken with the LSM780 microscope to define the accurate position of the FP. For quantification, the number of axons that exhibited turning contralaterally (crossing) or ipsilaterally, stalling or re-crossing/looping back in each imaging field were counted and presented as the percentage compared to the total number of vYFP-positive axons. Overshooting phenotypes were excluded from analysis, because we detected these phenotypes in the tissue areas damaged by electroporation and/or manipulation, even in shControl-targeted embryos.

The number of axons traced and scored was 3024 (from 34 embryos) for shControl-electroporated explants, 1475 (11 embryos) for shCyth1, 1032 (11 embryos) for shCyth2, 867 (7 embryos) for shCyth3, 456 (5 embryos) for shCyth1 + Cyth1-WT, 467 (6 embryos) for shCyth1 + Cyth1-E157K, 245 (4 embryos) for shCyth2 + Cyth2-WT, 377 (4 embryos) for shCyth2 + Cyth2-E156K, 411 (6 embryos) for shCyth3 + Cyth3-WT, 448 (5 embryos) for shCyth3 + Cyth3-E161K and 1543 (11 embryos) for shArf6.

### Supplemental References

- Guan, C. B., Xu, H. T., Jin, M., Yuan, X. B. and Poo, M. M.** (2007). Long-range  $\text{Ca}^{2+}$  signaling from growth cone to soma mediates reversal of neuronal migration induced by Slit-2. *Cell* **129**, 385–395.
- Halfter, W., Newgreen, D. F., Sauter, J. and Schwarz, U.** (1983). Oriented axon outgrowth from avian embryonic retinae in culture. *Dev Biol.* **95**, 56–64
- Harrington, A. W., St Hillaire, C., Zweifel, L. S., Glebova, N. O., Philippidou, P., Haleboua, S. and Ginty D. D.** (2011). Recruitment of actin modifiers to TrkA endosomes governs retrograde NGF signaling and survival. *Cell* **146**, 421–434.
- Li, J., Malaby, A. W., Famulok, M., Sabe, H., Lambright, D. G. and Hsu, V. W.** (2012). Grp1 plays a key role in linking insulin signaling to Glut4 recycling. *Dev. Cell* **22**, 1286–1298.
- Santy, L. C. and Casanova, J. E.** (2001). Activation of ARF6 by ARNO stimulates epithelial cell migration through downstream activation of both Rac1 and phospholipase D. *J. Cell. Biol.* **154**, 599–610.